Optical Materials: X 26 (2025) 100410

Contents lists available at ScienceDirect

Optical Materials: X

journal homepage: www.journals.elsevier.com/optical-materials-x

# Study of the effect of phase formation processes on the change in optical and thermal properties of $Nd_2Zr_2O_7$ ceramics with a pyrochlore structure

Artem L. Kozlovskiy [a,b,*], Dmitriy I. Shlimas [a], Natalya Volodina [a], Gulnaz ZhMoldabayeva [c], Mussa Kabiyev [a], Marina Konuhova [d]

[a] Engineering Profile Laboratory, L.N. Gumilyov Eurasian National University, Astana, 010008, Kazakhstan
[b] Department of General Physics, Satbayev University, Almaty, 050032, Kazakhstan
[c] Department Petroleum Engineering, Satbayev University, Almaty, 050013, Kazakhstan
[d] Institute of Solid State Physics University of Latvia, 8 Kengaraga str, LV-1063, Riga, Latvia

ARTICLE INFO

*Keywords:*
Vacancy defects
Absorption bands
Ceramic materials
Zirconates
Phase transformations
Rare earth elements

ABSTRACT

The paper presents the results of studies of the influence of phase formation processes with variations in annealing temperature on the processes of stabilization of the crystal structure, optical and thermal properties of $Nd_2Zr_2O_7$ ceramics, which have great potential for use in optoelectronic applications due to the transitions of $Nd^3$ ions, as well as high stability to external factors with the possibility of creating transparent ceramics. During the conducted studies it was established that the stabilization temperature of the $Nd_2Zr_2O_7$ phase is 1100–1250 °C, at which the throughput is maximum, and the thermal conductivity coefficient is about 2.1–2.2 W/m × K. The assessment of phase transformations and changes in optical properties revealed that an elevation in the annealing temperature, leading to stabilization of the $Nd_2Zr_2O_7$ phase, leads to a decrease in the concentration of oxygen vacancies in the structure of ceramics; however, at temperatures above 1200 °C, the observed growth in oxygen vacancies is due to the effects of substitution of $Zr^{4+}$ cations by $Nd^{3+}$ cations, which results in formation of additional oxygen vacancies in the structure, alongside impurity inclusions in the form of a cubic phase of Zr(Nd)$O_2$, which is a product of phase polymorphic transformations during high-temperature annealing. Alterations in the thermophysical properties of $Nd_2Zr_2O_7$ ceramics are directly dependent on phase formation processes and associated changes in the concentration of oxygen vacancies, which are the determining factor influencing the heat transfer rate.

## 1. Introduction

Interest in ceramics based on zirconates ($Gd_2Zr_2O_7$, $Nd_2Zr_2O_7$, $Sm_2Zr_2O_7$), which have a structural motif of the pyrochlore type ($A_2B_2O_7$, where cation A is usually selected from the actinide series, and $Zr^{4+}$ is selected as cation B), is due to a combination of structural, mechanical, strength, optical and thermal properties, opening up the possibility of using them as catalysts, inert matrix materials for dispersed nuclear fuel, anode materials, etc. [1–5]. The expansion of the potential for the use of ceramic materials is primarily associated with the combination of their properties, which in most cases play a decisive role in assessing the scope of application [4,5]. An important role in determining the potential use of ceramics based on zirconates or zirconium dioxide is played by their properties and phase composition, which has features associated with polymorphic transformations that depend on both temperature and external influences [5–8]. Moreover, the structural features of zirconates are determined not only by the structural motif (pyrochlore or fluorite), but also by concentration effects associated with the accumulation of vacancies in the structure of ceramics, the presence of which is due to cation substitution [9–13]. It should be noted that the presence of oxygen vacancies in the structure of ceramics plays not only a decisive role in the processes of electrical neutrality maintenance [14–16], but also in determination of optical and thermal properties, since the dielectric nature of ceramics directly depends on factors associated with the presence of point and vacancy defects [16–19]. The presence of a large number of oxygen vacancies in the

This paper was presented at the 12th International Conference on Luminescent Detectors and Transformers of Ionizing Radiation (LUMDETR), June 16-21, 2024, Riga, Latvia.

* Corresponding author. Engineering Profile Laboratory, L.N. Gumilyov Eurasian National University, Astana, 010008, Kazakhstan.
*E-mail address:* kozlovskiy.a@inp.kz (A.L. Kozlovskiy).

https://doi.org/10.1016/j.omx.2025.100410
Received 23 December 2024; Received in revised form 20 January 2025; Accepted 19 February 2025
Available online 7 March 2025

structure of zirconates results in thermal conductivity reduction, which in turn causes a rise in thermal insulation characteristics, which opens up opportunities for creation of heat-protective barrier materials on their basis, used as sacrificial coatings that protect heat-resistant alloys from high-temperature exposure [20–23]. At the same time, the presence of rare earth cations in the composition of ceramics allows the creation of various luminophores based on these ceramics, which have good luminescence indicators in the visible light and near IR range, which can be used in optical detectors, sensors, etc. [24–27]. It should be noted that these ceramics are among the promising materials with the possibility of using them in extreme conditions, including high temperatures that can lead to corrosion processes, high-dose radiation exposure, mechanical impact associated with external pressures, friction, etc. [28–30].

Interest in this type of ceramics, despite the large number of experimental works related to their production, the study of the prospects for modification by adding various stabilizing components [31–33], does not wane in view of the possibility of expanding the potential for the use of these ceramics, as well as the possibility of reducing the cost of manufacturing ceramics by simplifying the procedures for manufacturing ceramics. It should be noted that the choice of the method for production of ceramics, which determines the possibilities of controlling their properties, plays an important role in determining the potential for using zirconate-based ceramics as materials for nuclear applications, including the possibility of using them as inert matrix materials, thermal insulation materials, and materials for storing spent nuclear fuel [34–38]. A major role in determination of the kinetics of alterations in the properties of materials, especially optical and thermal characteristics, is played by the concentration dependences of oxygen vacancies, the formation of which in zirconates is associated with the need to maintain electroneutrality at substitution of $Zr^{4+}$ cations by trivalent cations, which occurs as a result of phase transformation processes, as well as during the formation of impurity inclusions in the structure, the emergence of which can occur as a result of polymorphic transformations or recrystallization processes. Based on the above, the main aim of this work is to determine the prospects for using the method of mechanical activation followed by thermal sintering of ground powders to control the phase composition, optical and thermal properties of ceramics based on zirconates, which have great potential for use in nuclear power engineering as materials for inert matrices of dispersed nuclear fuel, the creation of optical amplifiers for lasers, and also as high-temperature insulating optical materials that can be used in extreme conditions.

## 2. Materials and methods

The synthesis of ceramics was carried out using a fairly simple and inexpensive method of mechanical activation followed by thermal annealing of the ground powders under various conditions, the change of which is due to the need for the processes of initialization of phase transformations in ceramics, as well as their structural ordering due to thermal relaxation of deformation distortions caused by mechanical impact during grinding. Neodymium oxide ($Nd_2O_3$) and zirconium dioxide ($ZrO_2$) powders purchased from Sigma Aldrich were used to obtain ceramics; the chemical purity of the obtained samples was 99.95 %. Mechanical activation of the powders in order to obtain a homogeneous mixture was carried out using a PULVERISETTE 6 planetary mill (Fritsch, Berlin, Germany), the principle of which is based on the impact action of grinding balls in a grinding cup on the powders being ground in an equal stoichiometric ratio. The grinding speed is about 250–400 rpm, the grinding time is about 30 min. The choice of the grinding speed is determined by the possibility of crushing the initial grains and obtaining powders of uniform composition, while the grinding time of 30 min was chosen in order to prevent the formation of the effect of cold welding of the samples on the walls of the grinding cup. The use of the selected grinding conditions made it possible to obtain powders with an isotropic grain size, as well as a uniform distribution of elements in the composition, which subsequently contributed to the sintering of the samples under thermal exposure.

The grinding bodies are 10 mm diameter tungsten carbide balls, the grinding cup is an 80 ml tungsten carbide cup, which allows for about 20–40 g of ground powder to be obtained at a time with one load.

Annealing of ceramic samples was carried out in a Nabertherm LE 4/11/R6 muffle furnace (Nabertherm, Lilienthal, Germany). The heating rate of the samples to the specified temperature was 20 °C/min, holding at the specified temperature was about 5 h, after which the samples were slowly cooled together with the furnace until its complete cooling, which occurred in 10–20 h depending on the annealing temperature. The annealing temperature range was from 600 to 1400 °C. The choice of the annealing temperature range for the samples is determined by the possibilities of modeling the processes of phase transformations in the selected samples, while the upper limit of the annealing temperature was established a priori, as a result of experiments, according to which it was established that thermal annealing at temperatures above 1400 °C results in vitrification of the obtained ceramics and a large loss of mass as a result of thermal evaporation of the samples, which does not allow obtaining a stabilized phase.

A Phenom™ ProX scanning electron microscope (Thermo Fisher Scientific, Eindhoven, the Netherlands) was used to obtain images of the ceramics under study depending on the annealing temperature in order to study the morphological features. The samples were photographed in scanning mode at an accelerating voltage of 15 kV and a working segment of about 7.3–7.4 mm. The images were obtained at a magnification of about 25–30 k.

The study of the structural features of ceramics, the change of which is caused by phase formation processes when changing synthesis conditions, as well as by variations in the concentration of stabilizing additives, was carried out using the X-ray diffraction method. The diffraction patterns were obtained using a D8 ADVANCE ECO X-ray diffractometer (Bruker, Karlsruhe, Germany). The diffraction patterns were recorded in the Bragg-Brentano geometry, in the angular range of $2\theta = 20–100^{\circ}$, the recording step was $0.03^{\circ}$, the acquisition time at a point was 1 s.

The processing of X-ray diffraction patterns was carried out using the DiffracEVA v.4.2 software code. The parameters were refined by comparative analysis of the position of diffraction peaks with reference values from the PDF-2 database. The determination of the weight contributions of each established phase was carried out by determining the intensities and areas of reflections for each established phase taking into account the corundum numbers, which together made it possible to establish the weight contribution of each phase with sufficiently high accuracy (at least 0.1 wt %), which made it possible to compare changes in the phase composition of ceramics with variations in synthesis conditions, in particular, changes in the annealing temperature. The results of the phase composition of the studied ceramics were calculated based on the weight contributions of the observed reflexes for each of the established phases in the composition, followed by the calculation of their weight value taking into account the corundum numbers. The measurement error was determined using standard methods.

To confirm the structural changes in $Nd_2Zr_2O_7$ ceramics depending on the conditions of their synthesis, the Raman spectroscopy method was used, implemented using the Enspectr M532 Raman spectrometer (Spectr-M LLC, Chernogolovka, Russia).

The optical properties of Nd2Zr2O7 ceramics were studied using UV spectroscopy methods, implemented using a SPECORD 200/210/250 PLUS UV spectrophotometer (Analytik Jena, Jena, Germany). The spectra were obtained using an integral sphere. The measurement range was from 190 to 1000 nm, the measurement step was 1 nm, the time of spectrum acquisition at a point was 1 s. The measurement results were transmission spectra and absorption spectra, the general analysis of which made it possible to establish the relationship between phase changes and optical properties of ceramics.

The thermophysical parameters were determined by measuring the thermal conductivity coefficient, measured according to the method of longitudinal heat flow changes. The universal thermal conductivity meter KIT-800 (KB Teplofon, Russia) was used for the measurements.

The hardness was determined using the Vickers method, where a diamond pyramid was used as an indenter, and measurements were taken by indenting the pyramid at a given load into the surface of a ceramic sample, holding it for a certain time at a given load, and then evaluating the shape of the indenter imprint, as well as determining its diagonals to calculate the hardness values. The measurements were performed using the LM 700 microhardness tester (LECO, St. Joseph, USA). The measurements were performed with an indenter load of 100 N, and the indenter was held under load for about 30 s.

## 3. Results and discussion

Interest in zirconate-based ceramics is primarily due to their great potential for use in nuclear and alternative energy, which is due to a combination of their properties associated with high resistance to external influences (mechanical damage, pressure, corrosion processes when interacting with aggressive environments or exposure to high temperatures), thermophysical parameters, which give zirconates an advantage over other types of oxide ceramics, including $ZrO_2$ ceramics, as well as good compatibility with most types of structural materials used in nuclear energy [39–42]. At the same time, one of the determining parameters in the area of application is the method of manufacturing ceramics, which determines the cost of their manufacture and, as a consequence, determines the cost of their operation. The simplest and most inexpensive method of manufacturing composite ceramics using fairly simple procedures that do not require large expenditures is the method of mechanical activation, the main principle of which is the mechanical grinding of the initial components of ceramics with their subsequent heat treatment, the use of which allows initiating the processes of phase transformations, as well as controlling the concentration of structural defects and oxygen vacancies in the ceramic material, which play one of the key roles in determining the potential for use, as well as changing the strength and thermal parameters. In this case, the change in the mechanical activation conditions associated with the change in the grinding speed can be used to vary the change in the sizes of ceramics or to elevate the homogeneity degree of sizes, but in some cases, the grinding speed growth can lead to the occurrence of the effect of cold welding of powders on the walls of the grinding cup, which results in the grinding efficiency reduction, and as a consequence, the heterogeneity of the composition of the resulting ceramics, which is a very critical parameter in the production of composite ceramics obtained from two or more components [43].

Fig. 1 demonstrates the results of changes in the morphological features of the synthesized ceramics depending on the annealing

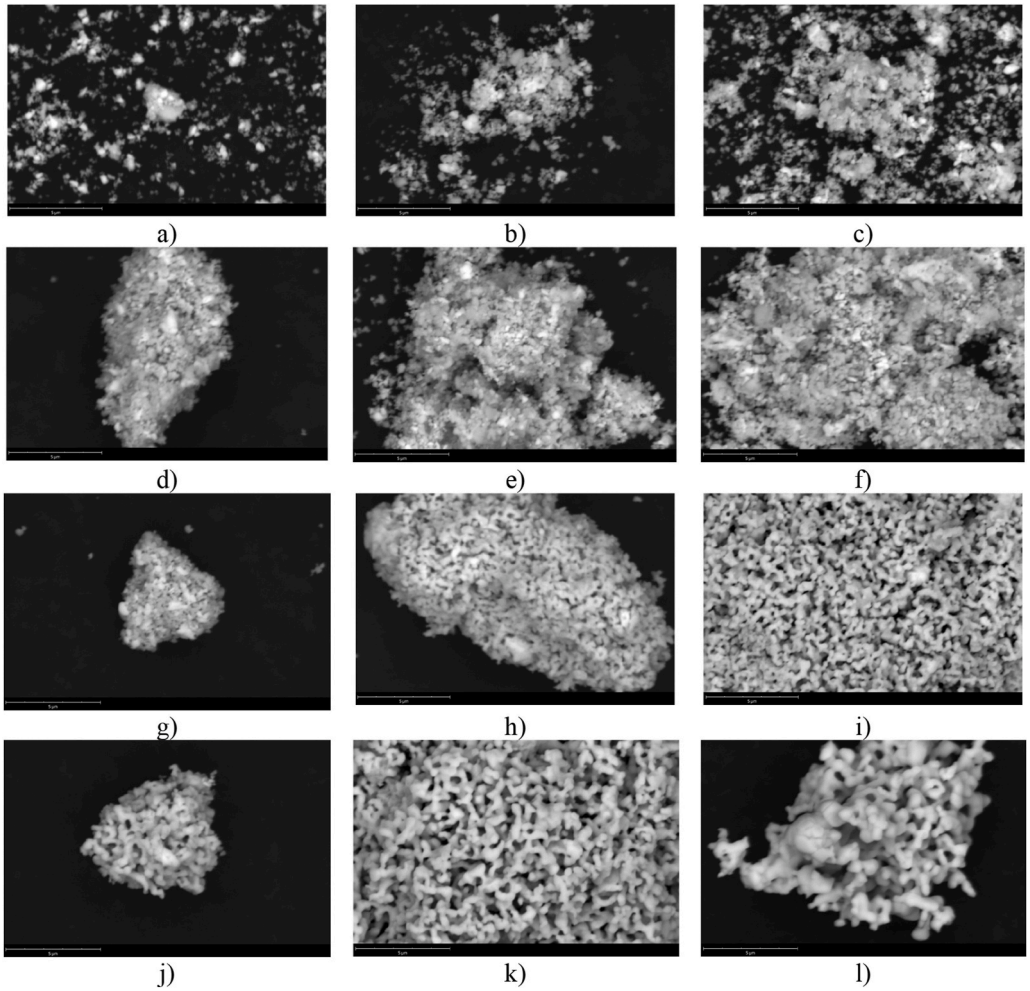


**Fig. 1.** Results of morphological features of synthesized ceramics depending on the annealing temperature: a) initial; b) annealed at a temperature of 600 °C; c) annealed at a temperature of 700 °C; d) annealed at a temperature of 800 °C; e) annealed at a temperature of 900 °C; f) annealed at a temperature of 1000 °C; g) annealed at a temperature of 1100 °C; h) annealed at a temperature of 1200 °C; i) annealed at a temperature of 1250 °C; j) annealed at a temperature of 1300 °C; k) annealed at a temperature of 1350 °C; l) annealed at a temperature of 1400 °C.

temperature, the alteration of which results in structural ordering associated with both the enlargement of particle sizes, their agglomeration and subsequent transformation associated with phase formation processes. The powder images were obtained using the scanning electron microscopy method, the samples were previously dispersed on holders in order to obtain a uniform distribution of powders on the carbon holder, which was used to fix the samples. The general appearance of the studied powders in the initial state after mechanical activation is a finely dispersed fraction of deformed particles that do not have a uniform shape, which is due to the mechanical crushing of the powders by grinding balls during the grinding process. At the same time, some of the grains agglomerate into larger inclusions, the presence of which indicates that in the case of the selected synthesis conditions, a cold welding effect is observed, but the number of large grains is small in relation to the finely dispersed fraction.

The result of thermal action on ground ceramic samples is expressed in the agglomeration of deformed grains into spherical particles, the dimensions of which are about 200–250 nm, while these particles agglomerate into larger agglomerations of grains with the annealing temperature growth.

The most significant changes in the morphological features in the studied ceramic samples are observed at annealing temperatures of 1100–1200 °C, at which grain coarsening is observed, with the formation of a dendritic structure, which is an agglomeration of particles connected along one or two edges, of an elongated oblong shape (see data in Fig. 1f and g). With a further increase in the annealing temperature above 1200 °C, particle coarsening is observed, as well as the formation of large spherical or diamond-shaped grains, the formation of which may be due to effects associated with phase transformations or polymorphic transformations that occur at high annealing temperatures. It should also be noted that the observed general trend of changes in the shape and size of grains indicates that at low annealing temperatures (below 1000–1100 °C) the main changes are associated with structural ordering, which in the case of morphological features manifests itself in the form of grain compaction, loss of the feather-like disordered structure, the presence of which is due to crushing processes. At temperatures above 1100 °C, the observed changes associated with the coarsening of grains, as well as the release of a coarse-grained fraction, indicate possible phase formation processes that occur as a result of thermal processes, which can be confirmed by the results of X-ray phase analysis.

Fig. 2 demonstrates X-ray diffraction patterns of the studied ceramic samples obtained as a result of the annealing temperature variation, the change of which was chosen in order to determine the phase transformations kinetics in $Nd_2O_3$ – $ZrO_2$ compounds, the ultimate goal of which is the formation of the $Nd_2Zr_2O_7$ phase, characteristic of the zirconate structure. The general appearance of the presented data on the X-ray diffraction patterns of the studied ceramics depending on the annealing temperature indicates three clearly expressed processes of structural changes caused by the influence of the annealing temperature.

The first changes observed in the diffraction patterns are associated with structural ordering processes, which are expressed in a change in the intensity and shape of the diffraction maxima of annealed samples at temperatures of 600–1000 °C in comparison with the data presented for the sample after mechanical activation, for which the shape and intensity of the diffraction reflections of the observed phases correspond to a strongly deformed structure of $Nd_2O_3$ oxides with a hexagonal type of crystal lattice and a monoclinic phase of $ZrO_2$. With an elevation in the annealing temperature in this temperature range, the observed changes in the intensities of the diffraction reflections indicate a growth in the structural ordering degree (crystallinity degree), while the general analysis of the diffraction patterns at these annealing temperatures did not reveal the formation of any diffraction reflections characteristic of the appearance of new phases or polymorphic transformations associated with the transformation of the monoclinic phase of zirconium dioxide into tetragonal or cubic, as well as reflections characteristic of the zirconate phase with a pyrochlore structure.

The second stage of structural changes observed in X-ray diffraction patterns is observed at temperatures of 1000–1300 °C, for which the formation of $Nd_2Zr_2O_7$ (PDF-01-083-4375) cubic phase in the ceramic structure is observed, spatial syngony Fm-3m(225), characterized by the pyrochlore structure. The observed changes in the intensity of diffraction reflections of the studied samples at annealing temperatures above 1000 °C are primarily due to phase transformation processes that arise as a result of exposure to high temperatures, leading to the formation of the main phase $Nd_2Zr_2O_7$ in the composition of ceramics with its subsequent dominance. The observed changes are also due to texturing effects arising from changes in phase composition and size effects associated with sintering and transformation processes. In this case, the

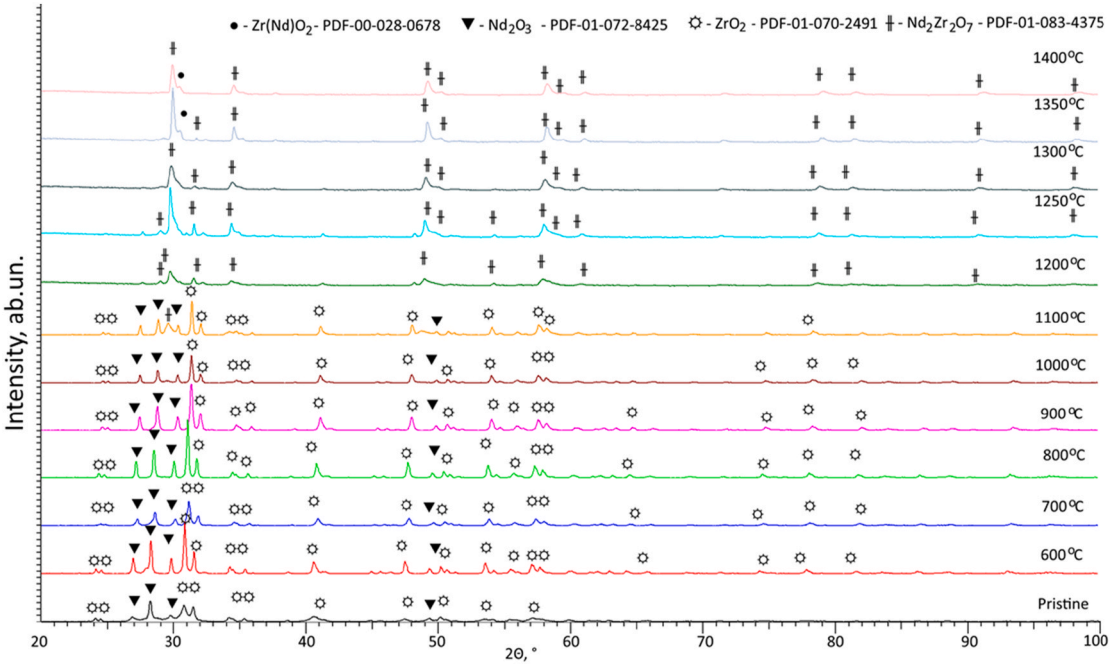


**Fig. 2.** Results of X-ray diffraction of the studied ceramics depending on the annealing temperature of the samples.

formation of this phase is observed at temperatures of 1000 °C, and complete transformation occurs at temperatures of 1200 °C. In the case of growth of the annealing temperatures above 1300 °C, the formation of inclusions in the form of a cubic phase of $Zr(Nd)O_2$ is observed in the structure of the ceramics, the appearance of which with a subsequent growth in the contribution to the composition of the ceramics can be explained by the effects of polymorphic transformations of the *m*-$ZrO_2$ → $Zr(Nd)O_2$ type, the initialization of which can explain the presence of large rhombohedral grains in the composition of the ceramics observed in the micrographs presented in Fig. 1j–l.

Fig. 3 illustrates the assessment results of changes in the weight contributions of the established phases in ceramics obtained from a mixture of $Nd_2O_3$ – $ZrO_2$ compounds with variations in the annealing temperature. The weight contributions of the established phases in the composition of the ceramics were determined using the method of determination of the specific gravity of the intensities of the diffraction reflections of each established phase, considering the corundum numbers, with subsequent calculation of the proportion of each phase in the sample and its normalization to 100 %. The presented insert in Fig. 3a of the X-ray diffraction patterns in the region of 2θ = 27–32° reflects the kinetics of phase transformations associated with thermal exposure to mechanically activated powders, and also reflects changes associated with structural ordering, characterizing the change in structural parameters as a result of thermal exposure. According to the given changes in the intensities and shape of diffraction reflections in Fig. 3a, it is possible to trace the main stages of phase transformations occurring in ceramics, caused by thermal action in the case of a change in temperature. The results presented in Fig. 3b reflect a change in weight contributions, the analysis of which can show how exactly the phase formation processes occur in ceramics.

Table 1 shows the evaluation results of the structural parameters (parameters and volume of the crystal lattice) for all identified phases in the composition of ceramics depending on the variation of the annealing temperature.

An analysis of the change in structural parameters for all established phases in the composition of ceramics depending on changes in the conditions of thermal annealing makes it possible to draw a conclusion about a change in the structural ordering degree associated with changes in the parameters and volume of the crystal lattice, as well as substitution effects that arise during thermal action on ground powders, an increase in the intensity of which leads to the formation of a cubic phase of $Nd_2Zr_2O_7$ at temperatures above 1000 °C.

Fig. 4 illustrates the results of Raman spectroscopy of the studied ceramic samples depending on the annealing temperature of the samples, which are presented to confirm the observed phase transformations in the $Nd_2O_3$ – $ZrO_2$ system at alteration of the thermal exposure conditions. From the data presented, during analysis of the spectra, it is evident that at annealing temperatures in the range of 600–1100 °C, the modes indicating the monoclinic phase of $ZrO_2$ dominate, and at temperatures of 1300, 1350 and 1400 °C, the $Nd_2Zr_2O_7$ modes have a higher intensity. The spectra of the unannealed sample contain 13 modes related to the monoclinic phase of zirconium oxide: 177 ($B_g$), 189 ($A_g$), 220 ($B_g$), 303 ($A_g$), 332 ($B_g$), 344 ($A_g$), 379 ($B_g$), 473 ($A_g$), 502 ($B_g$), 535 ($B_g$), 558 ($A_g$), 615 ($B_g$) and 635 ($A_g$) $cm^{-1}$; as well as a mode at 430 ($E_g$) $cm^{-1}$, which can be associated with $Nd_2O_3$ [44]. The spectra of the samples annealed at temperatures of 600–1100 °C differ only slightly; all these spectra contain 14 modes indicating the monoclinic phase of zirconium oxide, including 6 $A_g$ modes (at 189, 304, 344, 474, 559 and 633 $cm^{-1}$) and 8 $B_g$ modes (at 177, 221, 332, 380, 507, 532, 615 and 753 $cm^{-1}$), as well as one mode at 433 cm-1, which can be attributed to $Nd_2O_3$. Compared with the spectrum of the unannealed sample, the samples obtained at low temperatures have more intense peaks in the region of 500–600 $cm^{-1}$, as well as an additional peak at 452 $cm^{-1}$. Starting from the temperature of 1200 °C, an increase in the intensity of the peak at 305 $cm^{-1}$ is observed, which is related to the $E_g$ mode of the $Nd_2Zr_2O_7$ compound. At an annealing temperature of 1300 °C, the peaks associated with *m*-$ZrO_2$ become significantly less intense compared to the $E_g$ mode of the $Nd_2Zr_2O_7$ phase. The obtained results confirm the observed phase transformations in the ceramic samples obtained using the X-ray diffraction method.

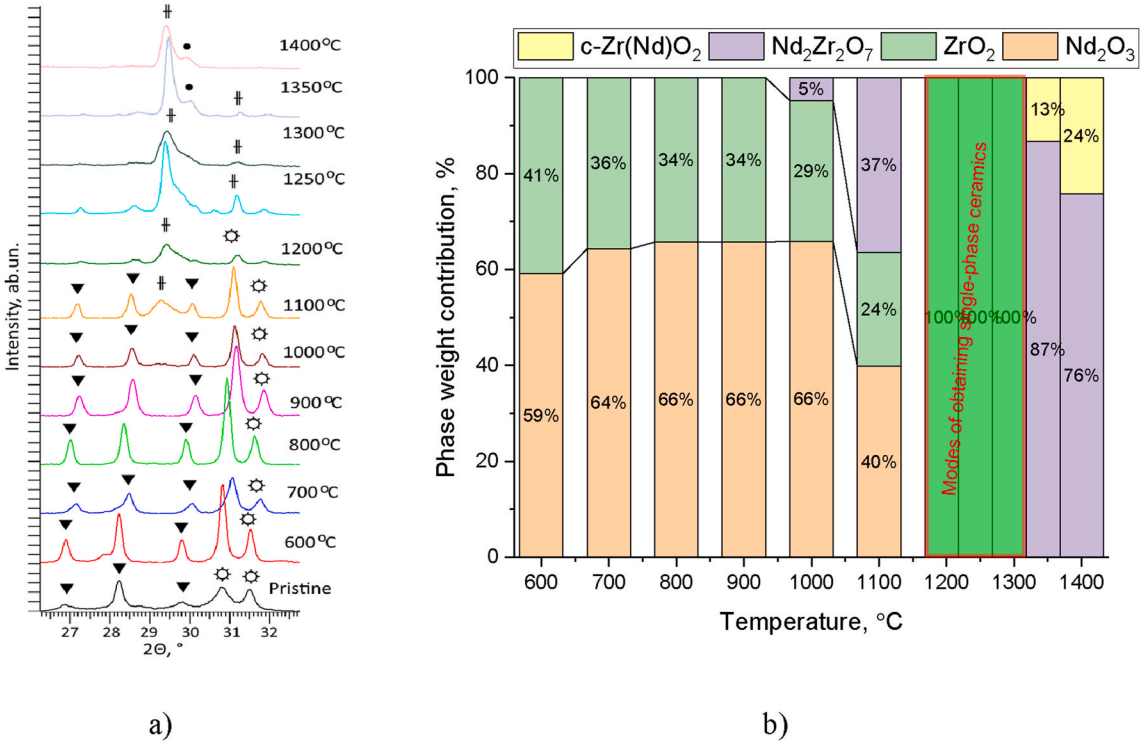


**Fig. 3.** Results of X-ray phase analysis: a) Detailed area 2θ = 27–32°, reflecting the main phase changes in ceramics with variation of annealing temperature; b) Results of evaluation of weight contributions of established phases in samples depending on annealing temperature.

**Table 1**
Structural parameter data.

| Temperature, °C | Structural parameters | | | |
|---|---|---|---|---|
| | $Nd_2O_3$ – hexagonal | $ZrO_2$ – monoclinic | $Nd_2Zr_2O_7$ – cubic | $Zr(Nd)O_2$ – cubic |
| Pristine | a = 3.8248 Å, c = 5.9872 Å, V = 75.85 Å$^3$ | a = 5.1386 Å, b = 5.2035 Å, c = 5.3062 Å, β = 99.243°, V = 140.04 Å$^3$ | – | – |
| 600°C | a = 3.8282 Å, c = 5.9956 Å, V = 76.02 Å$^3$ | a = 5.1387 Å, b = 5.2056 Å, c = 5.3147 Å, β = 99.124°, V = 140.37 Å$^3$ | – | – |
| 700°C | a = 3.8058 Å, c = 5.9626 Å, V = 74.79 Å$^3$ | a = 5.1089 Å, b = 5.1794 Å, c = 5.2699 Å, β = 99.833°, V = 137.59 Å$^3$ | – | – |
| 800°C | a = 3.8255 Å, c = 5.9884 Å, V = 75.90 Å$^3$ | a = 5.1387 Å, b = 5.2035 Å, c = 5.3020 Å, β = 99.005°, V = 140.22 Å$^3$ | – | – |
| 900°C | a = 3.7948 Å, c = 5.9593 Å, V = 74.32 Å$^3$ | a = 5.0974 Å, b = 5.2004 Å, c = 5.2529 Å, β = 99.380°, V = 137.39 Å$^3$ | – | – |
| 1000°C | a = 3.8074 Å, c = 5.9663 Å, V = 74.90 Å$^3$ | a = 5.1035 Å, b = 5.1739 Å, c = 5.2803 Å, β = 99.150°, V = 138.16 Å$^3$ | a = 10.5972 Å, V = 1190.07 Å$^3$ | – |
| 1100°C | a = 3.8152 Å, c = 5.9899 Å, V = 75.53 Å$^3$ | a = 5.1668 Å, b = 5.2138 Å, c = 5.2782 Å, β = 99.534°, V = 140.22 Å$^3$ | a = 10.6158 Å, V = 1196.34 Å$^3$ | – |
| 1200°C | – | – | a = 10.6021 Å, V = 1191.71 Å$^3$ | – |
| 1250°C | – | – | a = 10.6161 Å, V = 1196.44 Å$^3$ | – |
| 1300°C | – | – | a = 10.6154 Å, V = 1196.22 Å$^3$ | – |
| 1350°C | – | – | a = 10.6184 Å, V = 1197.22 Å$^3$ | a = 5.2038 Å, V = 140.92 Å$^3$ |
| 1400°C | – | – | a = 10.6373 Å, V = 1203.63 Å$^3$ | a = 5.2252 Å, V = 142.66 Å$^3$ |

In the spectra of the samples obtained by annealing at 1400 °C, only the modes characteristic of $Nd_2Zr_2O_7$ can be seen: $E_g$ at 302 cm$^{-1}$, $F_{2g}$ at 400 and 584 cm$^{-1}$, $A_{1g}$ at 508 cm$^{-1}$. The $E_g$ mode is related to the O–Zr–O bending vibrations, the $F_{2g}$ mode to the Zr–O stretching vibrations, and the $A_{1g}$ mode can contain contributions from both the O–Zr–O bending vibrations and the Nd–O and Zr–O stretching vibrations [45,46], the presence of which can be explained by the formation of inclusions in the form of cubic $Zr(Nd)O_2$, which is characterized by a strongly broadened shape of the spectral lines [47].

Fig. 5 reveals the results of the dependences of the change in the optical transmission and absorption spectra of the studied $Nd_2Zr_2O_7$ ceramics depending on the annealing temperature, the change of which results in phase transformations in the ceramic samples.

The optical transmission spectra revealed in Fig. 5a have a characteristically pronounced line shape for rare earth oxides, the presence of which is characterized by a set of absorption bands of varying intensity

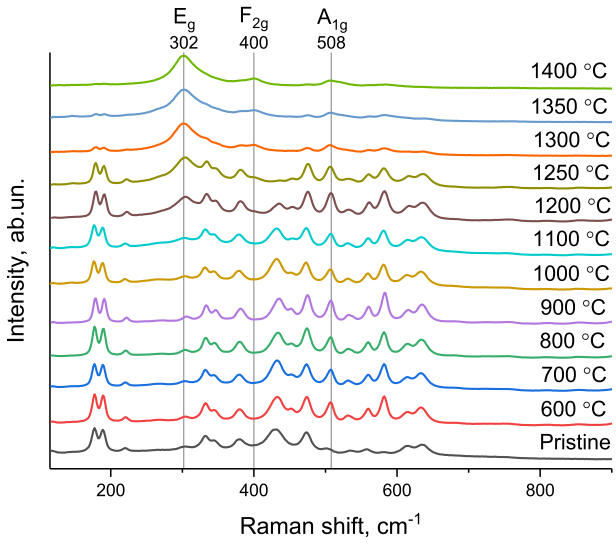


**Fig. 4.** Results of Raman spectroscopy of the studied ceramics depending on the annealing temperature.

in the visible and near IR ranges [48,49]. It should be noted that the change in the temperature of thermal annealing does not result in significant changes in the intensity and shape of the absorption bands in the transmission spectra, which in turn indicates the stability of these absorption centers in the structure of ceramics, as well as the preservation of their concentration regardless of structural changes associated with phase transformation processes, as well as changes in the weight contributions of oxide phases at low annealing temperatures (below 1000 °C).

An analysis of the optical absorption spectra of the studied ceramics depending on the annealing temperature showed the presence of a characteristic absorption band in the wavelength region in the range of 200–300 nm, characteristic of the presence of oxygen vacancies ($V_O$) in the structure of the ceramics, the presence of which is due to the structural features of $ZrO_2$. Moreover, the intensity of this absorption band is most intense for ceramic samples after mechanical activation, during which a large number of oxygen vacancies arise in the structure of the ceramics, the formation of which is caused by the mechanical-deformational effect on the crystalline structure during grinding and mixing of oxide components. In the case of thermal annealing, the intensity of this band decreases, which in turn is caused by processes associated with both structural ordering, the initialization of which, according to the data of structural analysis, occurs due to thermally stimulated relaxation of structural damage caused by mechanical activation, as well as phase transformations that are observed at temperatures above 1000 °C, for which the formation of the $Nd_2Zr_2O_7$ cubic phase is observed in the structure of ceramics. Moreover, the intensities of the absorption bands characteristic of rare earth compounds in the structure of the absorption spectra are preserved in the entire range of annealing temperatures, which indicates their resistance to thermal effects and phase transformation processes. It should be noted that in the case of the formation of $Nd_2Zr_2O_7$ and its dominance at temperatures of 1200–1300 °C, an increase in the intensity of the absorption band in the wavelength range of 200–300 nm is observed in the absorption spectra, the increase in the intensity of which, especially at temperatures above 1300 °C, can be explained by the processes of polymorphic transformations associated with the formation of inclusions in the form of a cubic phase of $Zr(Nd)O_2$, the formation of which is accompanied by the formation of oxygen vacancies, the concentration of which (according to the assessment of the change in the intensity of the band at 200–300 nm) is directly proportional to the weight contribution of the cubic phase of $Zr(Nd)O_2$. Thus, based on changes in the intensity of spectral lines characteristic of oxygen vacancies, the presence of which is associated

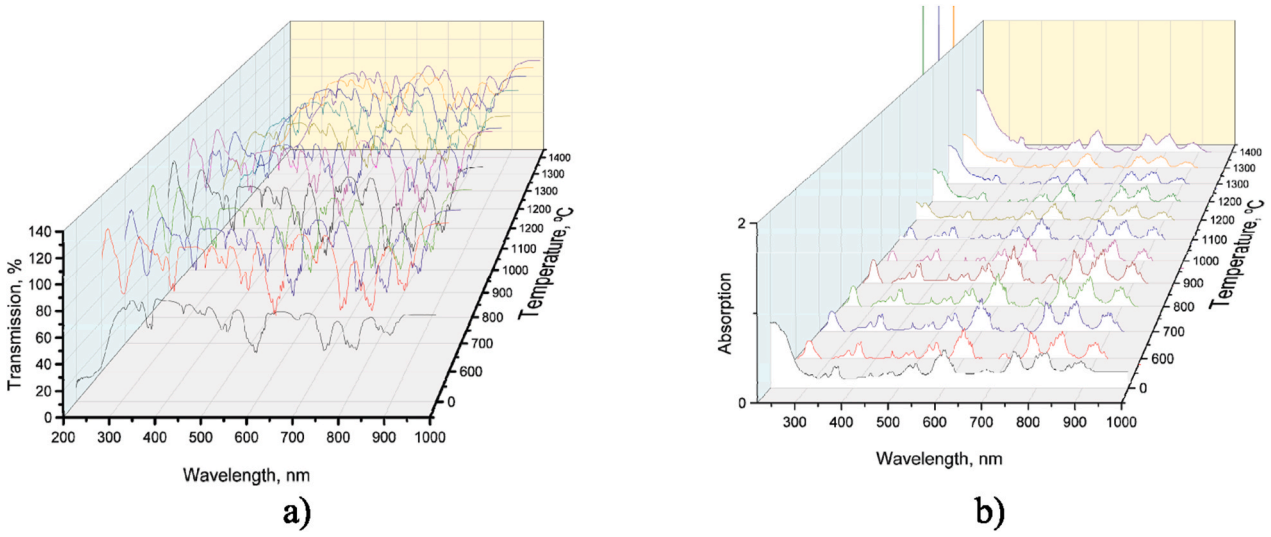


**Fig. 5.** Results of optical properties of ceramics depending on the annealing temperature: a) dependence of the change in transmission spectra; b) dependence of the change in absorption spectra.

with polymorphic transformations in zirconium dioxide, it is possible to judge the concentration of oxygen vacancies, the change of which is associated with both the structural ordering of zirconium dioxide and thermally induced polymorphic transformations in the composition of ceramics.

Fig. 6a illustrates the measurement results of the thermophysical parameters of the studied ceramics depending on the annealing temperature at which they were obtained, an alteration in which leads to the initialization of structural ordering processes (at temperatures of 600–1000 °C), as well as phase formation processes associated with the formation of the cubic phase of $Nd_2Zr_2O_7$ at temperatures above 1100 °C, and polymorphic transformations of the *m*-$ZrO_2$ → c- Zr(Nd)$O_2$ type, characteristic of annealing temperatures above 1300 °C.

In the case where the structure of ceramics contains two oxide phases – the hexagonal phase $Nd_2O_3$ and the monoclinic phase $ZrO_2$, the thermophysical parameters are determined by changes in the degree of structural ordering, as well as changes associated with a decrease in oxygen vacancies in the structure (see data in Fig. 6b). With a decrease in the concentration of oxygen vacancies in the structure of ceramics, according to the assessment of the intensity of spectral lines characteristic of oxygen vacancies, presented in Fig. 5b in combination with changes in the degree of structural ordering, the observed growth in thermal conductivity indicates an improvement in the thermophysical parameters, as well as the removal of barrier effects for phonon heat transfer during heating. The formation of a stable cubic phase of $Nd_2Zr_2O_7$ leads to an increase in the thermal conductivity coefficient of ceramics by approximately 40–43 % compared to the initial values of thermal conductivity, which are determined by the thermophysical properties of zirconium dioxide. However, the observed decrease in thermal conductivity for samples obtained at annealing temperatures above 1200 °C can be explained by the following factors. Structural ordering of the $Nd_2Zr_2O_7$ phase at higher temperatures can be accompanied by a change in the cation ratio, which in turn leads to the formation of additional oxygen vacancies, which is well confirmed by assessment of the observed changes in the intensity of spectral lines for oxygen vacancies presented in the optical absorption spectra of samples

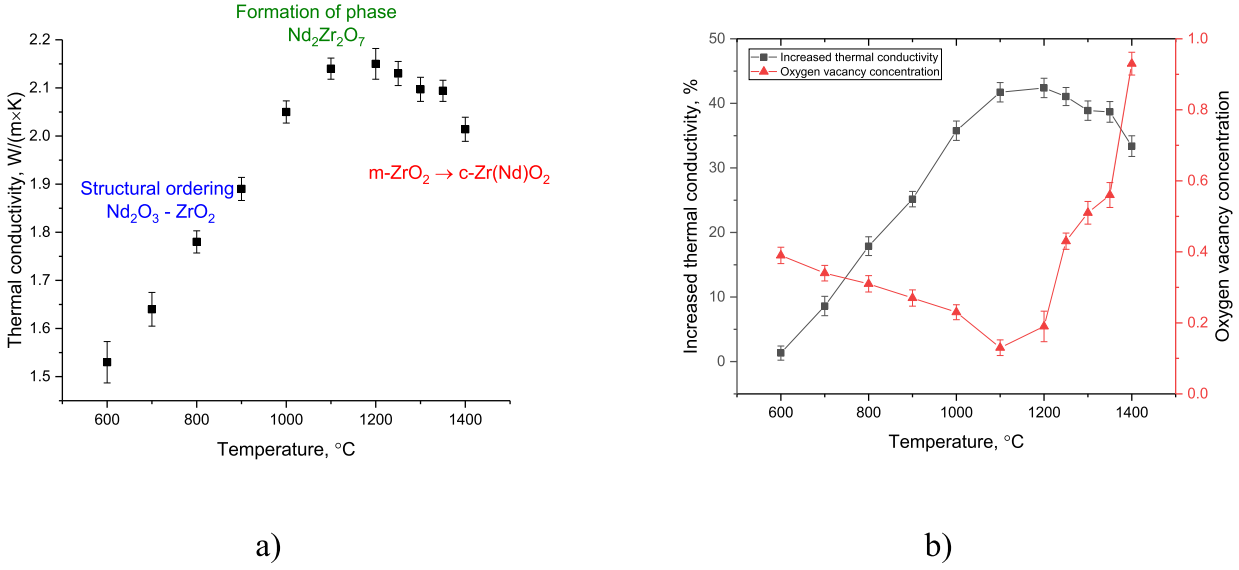


**Fig. 6.** Evaluation results of the thermophysical parameters of the studied ceramics: a) dependence of the change in the thermal conductivity coefficient of the studied ceramics on the sintering temperature; b) results of a comparative analysis of changes in the increase in thermal conductivity caused by structural ordering and phase formation processes and the concentration of oxygen vacancies, estimated based on the results of changes in the intensity of the absorption spectra.

annealed at temperatures above 1200 °C. Maintenance of the principle of electroneutrality in the crystal lattice at substitution of zirconium cations by neodymium cations leads to an increase in oxygen vacancies, which reduce the rate of heat transfer, thereby elevating heat loss in ceramics. Also, the formation of the cubic phase $Zr(Nd)O_2$ as a result of the initialization of polymorphic transformation processes at sintering temperatures above 1300 °C is accompanied by the formation of a large number of oxygen vacancies, which in turn negatively affects the thermal properties of ceramics.

The influence of phase formation processes on the mechanical properties of the ceramics under study was determined using indentation methods used to determine the hardness of ceramic samples and the single compression method used to assess the resistance of ceramics to single compression, i.e. determining the maximum pressure that ceramics can withstand during single compression. The assessment results of the strength characteristics depending on the annealing temperature are shown in Fig. 7.

The general trend of changes in the values of mechanical characteristics (hardness and maximum load) indicates a direct relationship between the structural ordering that occurs as a result of thermal annealing of ceramic samples with a change in the annealing temperature and the strength indicators. It should be noted that the formation of the $Nd_2Zr_2O_7$ cubic phase at temperatures above 1100 °C leads to a slowdown in the trends of change in hardness and the magnitude of the maximum load, from which it follows that the observed hardening effect in the annealing temperature range from 600 to 1100 °C is associated with changes in structural characteristics, as well as the relaxation of point and vacancy defects, the reduction of which was recorded using X-ray diffraction and Raman spectroscopy methods. Relaxation processes leading to a decrease in the concentration of structural defects in this case allow changing the hardness indices by a value of about 50–60 % in comparison with unannealed ceramics, and also increasing crack resistance by 25–30 %. Such a difference in the trends of hardening change for hardness and crack resistance is due to the fact that the hardness parameter characterizes the external impact at the same load, while when determining crack resistance, pressure is exerted on the sample with an increasing load, which in the case of porous ceramics leads to faster formation of cracks under compression. In this case, the formation of a stable $Nd_2Zr_2O_7$ phase, as well as subsequent polymorphic transformations of the $m$-$ZrO_2$ → c- $Zr(Nd)O_2$ type, arising as a result of the annealing temperature growth above 1300 °C, leads to a slowdown in the rate of hardening (the change in values is no more than 2 % for hardness values and no more than 5 % for crack resistance values), which indicates a small contribution from the presence of impurity inclusions associated with polymorphic transformations to the hardening of ceramics. Moreover, more pronounced changes in crack resistance values for samples obtained at temperatures above 1300 °C can be explained by changes in the morphological features of ceramics, which in this case increase the resistance to destruction of ceramics under external mechanical loads.

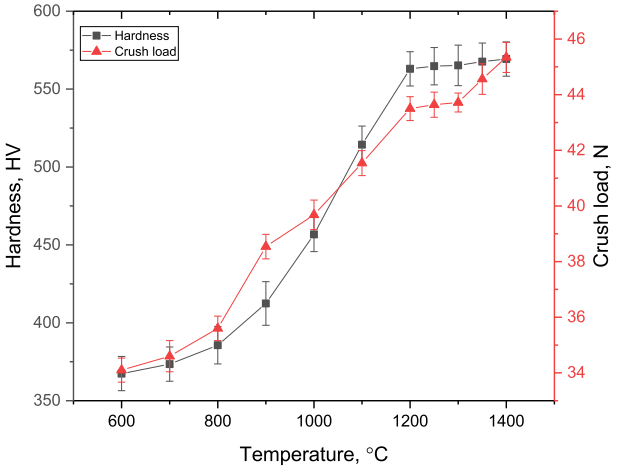


**Fig. 7.** Evaluation results of the mechanical characteristics of the studied ceramics depending on the annealing temperature, the change of which determines the processes of structural ordering and phase formation.

Analyzing the data obtained, it can be concluded that the most optimal parameters for obtaining single-phase $Nd_2Zr_2O_7$ ceramics with a cubic type of crystal structure, characteristic of pyrochlore, are temperatures of 1200–1250 °C, at which ceramics are obtained with high strength and thermal characteristics, as well as a sufficiently low concentration of oxygen vacancies in the composition, which allows them to be used as radiation-resistant materials for inert matrices.

## 4. Conclusion

In conclusion, the following results of the conducted studies characterizing the objects under study and also making it possible to establish the relationship between the synthesis conditions and changes in the properties of ceramics can be summarized.

An analysis of the morphological features of the synthesized ceramics, carried out using the scanning electron microscopy method, revealed the presence of changes in the shape and size of grains, characteristic of phase transformations associated with the processes of formation of $Nd_2Zr_2O_7$ with a pyrochlore structure, as well as polymorphic transformations of the m – $ZrO_2$ → $Zr(Nd)O_2$ type in the composition of ceramics at high temperatures above 1300 °C.

During assessment of the influence of variations in the sintering temperature in the two-component $Nd_2O_3$ – $ZrO_2$ system using the X-ray phase analysis method, the processes of phase transformations and structural ordering associated with the processes of thermal relaxation of structural distortions caused by grinding processes during mechanical activation were studied. During determination of the phase transformation kinetics in ceramics with a change in the annealing temperature, it was determined that the formation of the $Nd_2Zr_2O_7$ cubic phase occurs at an annealing temperature of 1000 °C, and complete structural formation is observed at a temperature of 1200 °C. At the same time, a growth in the annealing temperature above 1300 °C leads to the initialization of polymorphic transformations with the formation of a cubic phase of the $Zr(Nd)O_2$ type in the form of inclusions, the content of which is from 13 to 24 wt%.

Analysis of the change in the optical spectra of the studied ceramics depending on the annealing temperature showed the preservation of the main intensities of the absorption bands characteristic of the presence of rare earth elements in the ceramics, while the established dependence of the change in the concentration of oxygen vacancies made it possible to establish the main phase formation mechanisms in $Nd_2O_3$ – $ZrO_2$. During mechanical activation, the impact of grinding bodies on powders leads to deformation distortion of the structure, which is accompanied by the formation of a large number of oxygen vacancies, while in the case of low annealing temperatures of 600–1000 °C, the observed decrease in the intensity of the spectral line characteristic of the presence of oxygen vacancies in the structure indicates structural ordering and a decrease in the concentration of oxygen vacancies in the volume due to their annihilation. However, in the case of the formation of the $Nd_2Zr_2O_7$ cubic phase with its subsequent structural ordering, this leads to a growth in the intensity of the spectral line for oxygen vacancies, the elevation of which is due to the processes of substitution of $Zr^{4+}$ cations by trivalent $Nd^{3+}$ cations, as a result of which, in order to maintain electroneutrality, an oxygen vacancy is formed. At the same time, the initialization of the processes of phase polymorphic transformations of the $m$-$ZrO_2$ → c- $Zr(Nd)O_2$ type leads to a rise in the concentration of oxygen vacancies in the structure of ceramics due to additional effects of cation substitution in the $ZrO_2$ structure.

During the determination of the thermophysical parameters of $Nd_2Zr_2O_7$ ceramics depending on the annealing temperature and, as a

consequence, the initiated phase formation processes, a direct relationship between changes in the thermal conductivity coefficient and the concentration of oxygen vacancies in the structure of the ceramics, the change of which is due to the processes of both structural ordering and cation substitution, accompanied by the formation of additional vacancy defects while maintaining the electroneutrality of the crystal lattice, was established. It was determined that the formation of the c- Zr(Nd)$O_2$ phase at high annealing temperatures (above 1300 °C) leads to an increase in the concentration of oxygen vacancies, which in turn leads to a slowdown in heat exchange processes and, as a consequence, a decrease in the thermal conductivity of ceramics.

In the future, these ceramics will be considered as one of the candidate materials for use as materials for inert matrices of dispersed nuclear fuel, as well as structural materials for new-generation nuclear reactors capable of withstanding high temperatures and large doses of radiation. In the near future, experiments are planned to assess the resistance of ceramics to high-temperature irradiation, as well as to assess changes in structural parameters during the accumulation of radiation damage in the near-surface layer.

## CRediT authorship contribution statement

**Artem L. Kozlovskiy:** Writing – original draft, Visualization, Investigation, Funding acquisition, Data curation. **Dmitriy I. Shlimas:** Visualization, Resources, Methodology, Investigation, Formal analysis, Data curation. **Natalya Volodina:** Writing – original draft, Visualization, Validation, Software, Data curation, Conceptualization. **Gulnaz ZhMoldabayeva:** Writing – original draft, Methodology, Investigation, Formal analysis, Data curation, Conceptualization. **Mussa Kabiyev:** Visualization, Methodology, Investigation, Formal analysis. **Marina Konuhova:** Visualization, Validation, Resources, Investigation, Formal analysis, Data curation, Conceptualization.

## Funding

This research was funded by the Science Committee of the Ministry of Education and Science of the Republic of Kazakhstan (No. AP19574467). In addition, M. K was supported by EUROfusion Enabling Research Project ENR-MAT.02. ISSP-UL- "New dielectric functional materials and interfaces (DFMI) – Theoretical and Experimental analysis." This work has been carried out within the framework of the EUROfusion Consortium, funded by the European Union via the Euratom Research and Training Programme (Grant Agreement No 101052200 — EUROfusion). Views and opinions expressed are however those of the author(s) only and do not necessarily reflect those of the European Union or the European Commission. Neither the European Union nor the European Commission can be held responsible for them.

## Declaration of competing interest

The authors declare that they have no known competing financial interests or personal relationships that could have appeared to influence the work reported in this paper.

## Data availability

No data was used for the research described in the article.

## References

[1] S. Zinatloo-Ajabshir, M. Salavati-Niasari, Z. Zinatloo-Ajabshir, Nd2Zr2O7-Nd2O3 nanocomposites: new facile synthesis, characterization and investigation of photocatalytic behaviour, Mater. Lett. 180 (2016) 27–30.
[2] A.P. Anantharaman, Exploring the defect formation and ionic migration in A2Zr2O7 (A= La, Ce, Nd, and Gd) Pyrochlore solid-state electrolytes, Ceram. Int. 50 (22) (2024) 48116–48126.
[3] A. Kozlovskiy, Study of the influence of structural modification of ZrO2 ceramics on resistance to hydrogen absorption and gas swelling processes, International Journal of Mathematics and Physics 15 (2) (2024) 49–57.
[4] B. Qi, S. Liang, Y. Li, C. Zhou, H. Yu, J. Li, ZrO2 matrix toughened ceramic material-strength and toughness, Adv. Eng. Mater. 24 (6) (2022) 2101278.
[5] V.P. Savchyn, A.I. Popov, O.I. Aksimentyeva, H. Klym, Y.Y. Horbenko, V. Serga, A. Moskina, I. Karbovnyk, Cathodoluminescence characterization of polystyrene-BaZrO3 hybrid composites, Low Temp. Phys. 42 (7) (2016) 760–763.
[6] M. Konuhova, E. Kamolins, S. Orlova, A. Suleiko, R. Otankis, Optimisation of permanent magnets of bioreactor magnetic coupling while preserving their efficiency, Latv. J. Phys. Tech. Sci. 56 (4) (2019) 38–48.
[7] R.I. Shakirzyanov, N.O. Volodina, Y.A. Garanin, A.L. Kozlovskiy, D.I. Shlimas, K. K. Kadyrzhanov, M.V. Zdorovetz, Exploring the influence of sintering temperature on the phase composition, mechanical strength, and dielectric constant of porous ca-stabilized zirconium dioxide ceramics, Discover Materials 4 (1) (2024) 48.
[8] S.G. Giniyatova, A.L. Kozlovskiy, R.I. Shakirzyanov, N.O. Volodina, D.I. Shlimas, D. B. Borgekov, Structural, dielectric, and mechanical properties of high-content cubic zirconia ceramics obtained via solid-state synthesis, Appl. Sci. 13 (19) (2023) 10989.
[9] L. Wang, J. Li, H. Xie, Q. Chen, Y. Xie, Solubility, structure transition and chemical durability of Th-doped Nd2Zr2O7 pyrochlore, Prog. Nucl. Energy 137 (2021) 103774.
[10] S. Zinatloo-Ajabshir, Z. Zinatloo-Ajabshir, M. Salavati-Niasari, S. Bagheri, S.B. Abd Hamid, Facile preparation of Nd2Zr2O7–ZrO2 nanocomposites as an effective photocatalyst via a new route, J. Energy Chem. 26 (2) (2017) 315–323.
[11] H. Xie, R. Lan, L. Wang, Y. Ding, Preparation and chemical stability evaluation of new (Nd, An) 2Zr2O7-SrZrO3 multiphase ceramics, Journal of the Australian Ceramic Society 59 (3) (2023) 751–761.
[12] YuF. Zhukovskii, N. Pugno, A.I. Popov, C. Balasubramanian, S. Bellucci, Influence of F centres on structural and electronic properties of AlN single-walled nanotubes, J. Phys. Condens. Matter 19 (39) (2007) 395021.
[13] E.A. Kotomin, R.I. Eglitis, A.I. Popov, Charge distribution and optical properties of F+ and F centres in KNbO3 crystals, J. Phys. Condens. Matter 9 (22) (1997) L315–L321.
[14] D.B. Borgekov, A.T. Zhumazhanova, K.B. Kaliyekperova, S.B. Azambayev, A. L. Kozlovskiy, M. Konuhova, A.I. Popov, D.I. Shlimas, The effect of oxygen vacancies on the optical and thermophysical properties of (1-x)Si3N4 – xAl2O3 ceramics, Opt. Mater. 157 (2024) 116056.
[15] A.E. Ryskulov, I.A. Ivanov, A.L. Kozlovskiy, M. Konuhova, The effect of residual mechanical stresses and vacancy defects on the diffusion expansion of the damaged layer during irradiation of BeO ceramics, Opt. Mater. X 24 (2024) 100375.
[16] L. Wang, J. Li, H. Xie, Q. Chen, Y. Xie, Solubility, structure transition and chemical durability of Th-doped Nd2Zr2O7 pyrochlore, Prog. Nucl. Energy 137 (2021) 103774.
[17] L. Kong, I. Karatchevtseva, D.J. Gregg, M.G. Blackford, R. Holmes, G. Triani, Gd2Zr2O7 and Nd2Zr2O7 pyrochlore prepared by aqueous chemical synthesis, J. Eur. Ceram. Soc. 33 (15–16) (2013) 3273–3285.
[18] A.K. Alina, K.K. Kadyrzhanov, A.A. Kozlovskiy, M. Konuhova, A.I. Popov, D. D. Shlimas, D.B. Borgekov, WO3/ZnWO4 microcomposites with potential application in photocatalysis, Opt. Mater. 150 (2024) 115280.
[19] A.A. Prokhorov, L.F. Chernush, V. Babin, M. Buryi, D. Savchenko, J. Lancok, M. Nikl, A.D. Prokhorov, EPR and luminescence studies of the radiation induced Eu2+ centers in the $EuAl_3(BO_3)_4$ single crystals, Opt. Mater. 66 (2017) 428–433.
[20] R.I. Eglitis, M.M. Kuklja, E.A. Kotomin, A. Stashans, A.I. Popov, Semi-empirical simulations of the electron centers in MgO crystal, Comput. Mater. Sci. 5 (4) (1996) 298–306.
[21] M. Buryi, Z. Remes, V. Babin, A. Artemenko, S. Chertopalov, J. Micova, Cold plasma treatment of ZnO:Er nano- and microrods: the effect on luminescence and defects creation, J. Alloys Compd. 895 (2022) 162671.
[22] A.I. Popov, E.A. Kotomin, M.M. Kuklja, Quantum chemical calculations of the electron center diffusion in MgO crystals, Physica Status Solidi (B) Basic Research 195 (1) (1996) 61–66.
[23] Y. Zhang, M. Xie, F. Zhou, X. Cui, X. Lei, X. Song, S. An, Low thermal conductivity in La2Zr2O7 pyrochlore with A-site partially substituted with equimolar Yb2O3 and Er2O3, Ceram. Int. 40 (7) (2014) 9151–9157.
[24] J. Xiang, S. Chen, J. Huang, H. Zhang, X. Zhao, Phase structure and thermophysical properties of co-doped La2Zr2O7 ceramics for thermal barrier coatings, Ceram. Int. 38 (5) (2012) 3607–3612.
[25] J. Che, X. Liu, X. Wang, K.P. Furlan, S. Zhang, Influence of B-site substituent Ce on thermophysical, oxygen diffusion, and mechanical properties of La2Zr2O7, Ceram. Int. 49 (7) (2023) 10936–10945.
[26] M.A. Monge, R. Gonzalez, J.E. Munoz Santiuste, R. Pareja, Y. Chen, E.A. Kotomin, A.I. Popov, Photoconversion and dynamic hole recycling process in anion vacancies in neutron-irradiated MgO crystals, Phys. Rev. B Condens. Matter 60 (6) (1999) 3787–3791.
[27] E. Elsts, G. Krieke, U. Rogulis, K. Smits, A. Zolotarjovs, J. Jansons, A. Sarakovskis, K. Kundzins, Rare earth doped glass–ceramics containing NaLaF4 nanocrystals, Opt. Mater. 59 (2016) 130–135.
[28] K.K. Kumarbekov, A.B. Kakimov, Z.T. Karipbayev, M.T. Kassymzhanov, M.G. Brik, C.G. Ma, M. Piasecki, Y. Suchikova, M. Kemere, M. Konuhova, Temperature-dependent luminescence of europium-doped $Ga_2O_3$ ceramics, Opt. Mater. X 25 (2024) 100392.
[29] R. Stankeviciute, A. Zalga, Sol-gel synthesis, crystal structure, surface morphology, and optical properties of $Eu_2O_3$-doped $La_2Mo_3O_{12}$ ceramic, J. Therm. Anal. Calorim. 118 (2) (2014) 925–935.

[30] Z. Yang, Y. Li, W. Pan, C. Wan, Abnormal thermal expansion coefficients in (Nd 1-x Dy x) 2 Zr 2 O 7 pyrochlore: the effect of low-lying optical phonons, J. Adv. Ceram. 12 (5) (2023).
[31] A.L. Kozlovskiy, M.B. Kabiyev, D.I. Shlimas, V.V. Uglov, Study of the effect of the formation of two-phase ceramics based on neodymium zirconate due to doping with MgO and Y2O5 on the stability of strength and thermophysical parameters under irradiation, Eurasian Physical Technical Journal 21 (2) (2024) 5–13, 48.
[32] S.G. Giniyatova, N.A. Sailaukhanov, E. Nesterov, M.V. Zdorovets, A.L. Kozlovskiy, D.I. Shlimas, Research of structural, strength and thermal properties of ZrO2—CeO2 ceramics doped with yttrium, Crystals 12 (2) (2022) 242.
[33] S. Solomon, A. George, J. Thomas, A. John, Preparation, characterization, and ionic transport properties of nanoscale LnZrO (Ln= Ce, Pr, Nd, Sm, Gd, Dy, Er, and Yb) energy materials, J. Electron. Mater. 44 (1) (2015).
[34] S.K. Sharma, V. Grover, A.K. Tyagi, D.K. Avasthi, U.B. Singh, P.K. Kulriya, Probing the temperature effects in the radiation stability of Nd2Zr2O7 pyrochlore under swift ion irradiation, Materialia 6 (2019) 100317.
[35] M. Buryi, L. Havlak, V. Jary, J. Barta, V. Laguta, A. Beitlerova, J. Li, M. Nikl, Specific absorption in $Y_3Al_5O_{12}$:Eu ceramics and the role of stable $Eu^{2+}$in energy transfer processes, J. Mater. Chem. C 8 (26) (2020) 8823–8839.
[36] H. Ohtani, S. Matsumoto, B. Sundman, T. Sakuma, M. Hasebe, Equilibrium between fluorite and pyrochlore structures in the ZrO2–Nd2O3 system, Mater. Trans. 46 (6) (2005) 1167–1174.
[37] G. Krieke, A. Sarakovskis, M. Springis, Upconversion luminescence of a transparent glass ceramics with hexagonal Na(Gd,Lu)$F_4$ nanocrystals, J. Alloys Compd. 694 (2017) 952–958.
[38] U. Rogulis, E. Elsts, J. Jansons, A. Sarakovskis, G. Doke, A. Stunda, K. Kundzins, Rare earth activated oxyfluoride glasses and glass-ceramics for scintillation applications, IEEE Trans. Nucl. Sci. 59 (5 PART 2) (2012) 2201–2206, https://doi.org/10.1109/TNS.2012.2212724, 6316153.
[39] I. Kenzhina, Study of phase formation mechanisms in composite xSi3N4–(1-x) ZrO2 ceramics and their role in hardening of ceramics, International Journal of Mathematics and Physics 15 (2) (2024) 23–33.
[40] I.E. Kenzhina, A.L. Kozlovskiy, M. Begentayev, A. Tolenova, S. Askerbekov, Influence of the change of phase composition of (1−x) ZrO2–xAl2O3 ceramics on the resistance to hydrogen embrittlement, Materials 16 (22) (2023) 7072.
[41] A.L. Kozlovskiy, Study of the influence of the accumulated dose of damage in the near-surface layer on resistance to external influences associated with corrosion processes during high-temperature annealing, Eurasian Physical Technical Journal 21 (1) (2024).
[42] P. Shukla, T. Watanabe, J.C. Nino, J.S. Tulenko, S.R. Phillpot, Thermal transport properties of MgO and Nd2Zr2O7 pyrochlore by molecular dynamics simulation, J. Nucl. Mater. 380 (1–3) (2008) 1–7.
[43] A. Berar, M.A. Mureșan-Pop, L. Barbu-Tudoran, R. Barabas, L. Bizo, High-temperature solid-state synthesis of Mg-doped ZrO 2: structural, optical and morphological characterization, Stud. UBB Chem 2 (2020) 221–232.
[44] X. Zhao, D. Vanderbilt, Phonons and lattice dielectric properties of zirconia, Phys. Rev. B 65 (7) (2002) 075105.
[45] Y. Wang, B. Gao, Q. Wang, X. Li, Z. Su, A. Chang, A 2 Zr 2 O 7 (A= Nd, Sm, Gd, Yb) zirconate ceramics with pyrochlore-type structure for high-temperature negative temperature coefficient thermistor, J. Mater. Sci. 55 (2020) 15405–15414.
[46] P. Anithakumari, V. Grover, C. Nandi, K. Bhattacharyya, A.K. Tyagi, Utilizing non-stoichiometry in $Nd_2Zr_2O_7$ pyrochlore: exploring superior ionic conductors, RSC Adv. 6 (100) (2016) 97566–97579.
[47] A. Kumar, P. Kumar, A.S. Dhaliwal, Phase transformation behavior of Ca-doped zirconia sintered at different temperatures, J. Korean Ceram. Soc. 59 (3) (2022) 370–382.
[48] L. Havlak, V. Jary, J. Barta, M. Buryi, M. Rejman, V. Laguta, M. Nikl, Tunable $Eu^{2+}$ emission in $K_xNa_{1-x}LuS_2$ phosphors for white LED application, Mater. Des. 106 (2016) 363–370.
[49] A.B. Usseinov, A.T. Akilbekov, E.A. Kotomin, A.I. Popov, D.D. Seitov, K. A. Nekrasov, Z.T. Karipbayev, The first principles calculations of CO2 adsorption on (101¯ 0) ZnO surface, in: AIP Conference Proceedings, vol. 2174, AIP Publishing, 2019, December, 1.